

Cross-correlations of the Cosmic Neutrino Background: HR-DEMNUi simulation analysis

Beatriz Hernández-Molinero,¹ Matteo Calabrese,^{2,3} Carmelita Carbone,² Alessandro Greco,⁴ Raul Jimenez,^{5,6} Carlos Peña Garay,^{1,7}

¹Laboratorio Subterráneo de Canfranc, 22880 - Canfranc-Estación, Huesca, Spain.

²INAF – Istituto di Astrofisica Spaziale e Fisica cosmica di Milano (IASF-MI), Via Alfonso Corti 12, I-20133 Milano, Italy

³Astronomical Observatory of the Autonomous Region of the Aosta Valley (OAVdA), Loc. Lignan 39, I-11020, Nus (Aosta Valley), Italy

⁴Department of Astronomy, University of Florida, 211 Bryant Space Science Center, Gainesville, FL 32611, USA

⁵ICCUB, University of Barcelona, Martí i Franques 1, E-08028 Barcelona, Spain.

⁶Institució Catalana de Recerca i Estudis Avançats, Pg. Lluís Companys 23, Barcelona, E-08010, Spain.

⁷I2SysBio, CSIC-University of Valencia, 46071 - Valencia, Spain.

E-mail: bhernandez@lsc-canfranc.es, alessandro.greco.1@phd.unipd.it, calabrese@oavda.it, carmelita.carbone@inaf.it, raul.jimenez@icc.ub.edu, cpenya@lsc-canfranc.es

Abstract. We use the high-resolution HR-DEMNUi simulations to compute cross-correlations of the Cosmic Neutrino Background $C_{\nu B}$ with other observables, namely: cold dark matter density, effective weak lensing convergence, neutrino velocity and neutrino deflection angle. We provide, for the first time, this high-fidelity cross-correlation maps in order to illustrate how much can be learned from them once the cosmic neutrino background is measured. As cross-correlations will have more signal than auto-correlations of the $C_{\nu B}$ itself, these might be the ones to be measured first by Ptolemy-like experiments. Our predictions thus provide the imprint of what massive neutrinos should look like from cosmological observations.

Contents

1	Introduction	1
2	Methodology	2
3	Maps and power spectra	3
4	Cross-correlations	5
5	Conclusions	7

1 Introduction

The Cosmic Neutrino Background ($C_\nu B$), which carries information about the Universe from just one second after the big bang, has not yet been detected. However, some experiments are being designed and developed to achieve this, such as tritium capture table-top experiments such as Ptolemy [1]. Once measured, it will provide invaluable information about the early stages of the Universe and the nature of neutrinos [2–5].

In previous works [6, 7] we have shown how gravity modifies the helicity of neutrinos originating from the cosmic background. Changes in the cosmic neutrino helicity density due to gravity modify the expected cosmic neutrino background capture rates. Experiments sensitive to the $C_\nu B$ can unveil the nature of neutrinos, i.e., they can exploit the average capture rate to uncover the Dirac or Majorana particle nature of neutrinos. These experiments will detect only left-handed neutrinos if neutrinos are Dirac particles but they will be sensitive to both left- and right-handed neutrinos if those are Majorana particles [5, 6, 8]. Given the importance of this possible discovery, it is worth exploring in detail the possible angular dependence of this signal¹.

The study of cosmological signals is motivated by the current limits provided by cosmological surveys, which indicate that the sum of neutrino masses is very close to the total mass inferred from underground experiments that measure the mass splits, i.e., 0.059 eV [9]. This strongly suggests, within the framework of Bayesian evidence, that the hierarchy is normal [10, 11]. If this is the case, neutrinoless double-beta decay experiments [12, 13], which are the current experimental method to discover the nature of neutrinos, will need to operate in the several-ton range, which presents significant challenges. Given this scenario, cosmological signals emerge as a promising way to reveal the nature of neutrinos.

In order to explore the angular dependence of cosmic neutrino background signals we have produced full-sky maps of Cold Dark Matter (CDM), Weak Lensing (WL) convergence, neutrino density, neutrino velocity, and neutrino deflection angle along with all cross-correlations. We will demonstrate the angular dependence of these signals and identify where they are maximal. This, in turn, will provide clues for discovering the nature of neutrinos from observations of the sky.

¹The angular dependence could be obtained by installing several Ptolemy-like detectors around the globe, much like gravitational waves observatories, with the advantage that these tritium capture devices are table-top experiments [1].

The paper is organised as follows. In § 2 we present the HR-DEMNUi simulations used to produce the full sky maps, for both CDM and neutrinos, which are shown in § 3. All cross-correlations and auto-correlations maps and power spectra are gathered in § 4. Finally, the discussion and conclusions are addressed in § 5.

2 Methodology

In previous works [6, 7], we have shown how gravity modifies the helicity content of the cosmic neutrino background. The cosmic neutrino helicities are modified due to gravitational fields (mostly CDM) that deflect neutrinos when they travel nearby clustered structures. The helicity change can be calculated through the angle of deflection that neutrinos suffer throughout their path since decoupling one second after the big bang. Motivated by the possibility to measure this signal over the full sky and to compute its clustering properties, we show here the neutrino angle of deflection, $\cos \theta_\nu$, map of the full simulation. The deflection angle is calculated for each neutrino of the simulation as the change in each velocity vector from $z = 3$ down to $z = 0$ in the same way as it was done in [6, 7]. Furthermore, we have extended the computation of the deflection angle to include other observables, like the neutrino velocity field, WL maps and CDM density.

All maps have been produced from the “Dark Energy and Massive Neutrino Universe” (DEMNUi) suite of large N-body simulations [14]. The DEMNUi simulations have been produced with the aim of investigating the Large-Scale Structure (LSS) of the Universe in the presence of massive neutrinos and dynamical Dark Energy (DE), and they were conceived for the nonlinear analysis and modelling of different probes, including CDM, halo, and galaxy clustering [15–25], weak lensing, CMB lensing, Sunyaev-Zel’dovich and integrated Sachs-Wolfe effects [14, 26, 27], cosmic void statistics [28–32], as well as cross-correlations among these probes [33, 34].

In particular, we have used the new high-resolution (HR) simulations with 64 times better mass resolution than previous standard runs: the HR-DEMNUi simulations are characterised by a comoving volume of $(500 h^{-1} \text{Gpc})^3$ filled with 2048^3 CDM particles and, when present, 2048^3 neutrino particles. The simulations are initialised at $z_{\text{in}} = 99$ with Zel’dovich initial conditions. The initial power spectrum is rescaled to the initial redshift via the rescaling method developed in [35]. Initial conditions are then generated with a modified version of the `N-GenIC` software, assuming Rayleigh random amplitudes and uniform random phases. The HR-DEMNUi set consists of two simulations with total neutrino masses of $\sum m_\nu = 0, 0.16 \text{ eV}$ considered in the degenerate mass scenario with three active neutrinos. The other cosmological parameters of the simulations are based on a Planck 2013 [36] ΛCDM reference cosmology (with massless neutrinos), in particular: $n_s = 0.96$, $A_s = 2.1265 \times 10^{-9}$, $h = H_0/[100 \text{ km s}^{-1} \text{Mpc}^{-1}] = 0.67$, $\Omega_b = 0.05$, and $\Omega_m = \Omega_{\text{CDM}} + \Omega_b + \Omega_\nu = 0.32$; H_0 is the Hubble constant at the present time, n_s is the spectral index of the initial scalar perturbations, A_s is the scalar amplitude, Ω_b the baryon density parameter, Ω_m is the total matter density parameter, Ω_{CDM} the CDM density parameter, and Ω_ν the neutrino density parameter. In the presence of massive neutrinos, Ω_b and Ω_m are kept fixed to the above values, while Ω_{CDM} is changed accordingly. Tab. 1 summarises the masses of the CDM and neutrino particles together with the neutrino fraction $f_\nu \equiv \Omega_\nu/\Omega_m$.

The simulations employed in this study are those that account for neutrinos as massive particles with $\Sigma m_\nu = 0.16 \text{ eV}$.

HR-DEMNUi			
$\sum m_\nu$ [eV]	f_ν	$m_p^{\text{CDM}} [h^{-1}M_\odot]$	$m_p^\nu [h^{-1}M_\odot]$
0	0	1.2921×10^9	0
0.16	0.012	1.2767×10^9	1.5441×10^7

Table 1: Summary of particle masses and neutrino fractions implemented in the HR-DEMNUi simulations. The first column shows the total neutrino mass, the second the fraction of neutrinos and matter density parameters, and the last two columns show the corresponding mass of CDM and neutrino particles implemented in the simulations.

3 Maps and power spectra

The CDM and neutrino maps are obtained from the DM and neutrino particle distribution of the HR-DEMNUi simulation, once a full-sky lightcone has been created by means of a stacking technique of the comoving particle snapshots in spherical shells, with the observer placed at their centre. This procedure follows the approaches of [37, 38], and was developed to perform high-resolution CMB and weak lensing simulations [39, 40]. The standard way to build lightcones is to pile up high-resolution comoving snapshots within concentric cells to fill the lightcone to the maximum desired source redshift. With the observer placed at $z = 0$, the volume of the lightcone is sliced into full-sky spherical shells of the desired thickness in redshift. The surface mass density Σ on each sphere is defined on a two-dimensional grid. For each pixel of the i -th sphere, one has

$$\Sigma^{(i)}(\boldsymbol{\theta}) = \frac{n \cdot m_p}{A_{\text{pix}}}, \quad (3.1)$$

where n is the number of particles in the pixel, A_{pix} is the pixel area in steradians, and m_p is the particle mass of the N -body simulation in each pixel, either m_p^{CDM} or m_p^ν . All the particles distributed within each of these 3D matter shells are then projected onto 2D spherical maps, assigning a specific sky pixel to each particle via the HEALpix² [41] pixelization procedure. For this work, we have produced full-sky, surface mass density maps for CDM and neutrino particles independently, on a HEALpix grid with $n_{\text{side}} = 4096$, which corresponds to a pixel resolution of 0.85 arcmin. The full-sky density maps, of both CDM and neutrinos, have been constructed placing the observer at the centre of the simulation box at $z = 0$, considering a $250 \text{ Mpc } h^{-1}$ comoving radius around this central observer. If n particles fall into a particular pixel, the total mass at those coordinates will be $n \cdot m_p$. A similar method has been applied to build the catalogue for the neutrino velocity modulus and deflection angle, where the velocity and deflection angle have been calculated for each neutrino particle of the simulation: as in the case of the particle lightcones, given the particle position in the simulation, full-sky maps of neutrino velocity and deflection angle have been produced, representing the distribution of those quantities on a 2D HEALpix grid. In this case, the value returned in the full-sky map is the average over all particle velocities, or deflection angles, that fall into that pixel.

The corresponding maps for each of the above quantities are shown in the four panels of Figure 1. It is worth noting that in the left panels of Figure 1 the shown quantities are not

²<http://healpix.sourceforge.net>

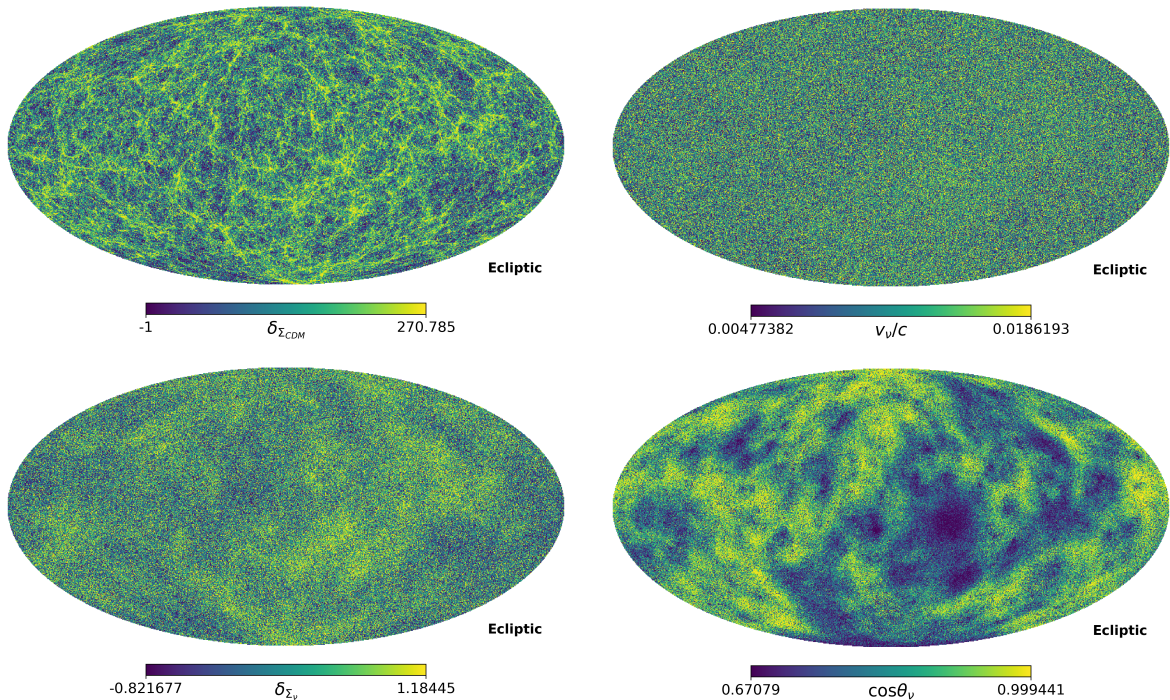


Figure 1: Full-sky map of $250h^{-1}\text{Mpc}$ comoving radius around an observer placed at the centre of CDM surface overdensity (top left), neutrino velocity modulus (top right), neutrino surface overdensity (bottom left), and neutrino mean cosine of deflection angle (bottom right).

the surface densities but δ_Σ , where $\delta_\Sigma \equiv (\Sigma - \bar{\Sigma})/\bar{\Sigma}$ is the density contrast, i.e. the surface density difference of each pixel over the mean surface density of all pixels.

Observing the the left panels of Figure 1, i.e. the distribution of $\delta_{\Sigma_{\text{CDM}}}$ and δ_{Σ_ν} , one can notice that neutrino clustering follows the CDM clustering, as neutrinos fall into the CDM potential wells. But, due to their hot thermal velocities, especially for low neutrino masses as $\Sigma m_\nu = 0.16$ eV, neutrino perturbations are much smaller than CDM ones and they cluster on much larger scales than CDM, ie only above their free streaming length, λ_{FS} . Therefore the δ_{Σ_ν} distribution appears much more diffused and smoother (as also the minimum and maximum values in the colour bars show) than the $\delta_{\Sigma_{\text{CDM}}}$ one, but in any case their correlation is observable from the maps. Instead, comparing the left and right bottom panels of Figure 1, ie the distributions of δ_{Σ_ν} and of $\cos\theta_\nu$, it looks like the two quantities are anticorrelated on large scales, ie that to more dense “brighter” regions in the neutrino overdensity there correspond “darker” regions where $\cos\theta_\nu$ assumes smaller values. Since, regions with a lower mean $\cos\theta_\nu$ correspond to larger angles of deflection, and since, as noticed above, δ_{Σ_ν} is correlated to $\delta_{\Sigma_{\text{CDM}}}$, this means that, in regions where the CDM overdensity is higher, the gravitational force will make neutrinos to deflect more. Finally, concerning the top left panel of Figure 1, it is difficult to identify any structure in the distribution of the neutrino velocity modulus, probably because the contribution of coherent neutrino velocities is very small and hidden by their thermal velocity which is dominant especially of the low neutrino masses considered. In Figure 2 we show the corresponding auto-correlations (the diagonal panels) as well as the cross-correlations (the off-diagonal panels). All these angular correlation in the spherical harmonic domain have been obtained applying to the maps the routine `anafast` of

the HEALpix package [41]. Because we have a single cosmological realisation and in order to reduce the noise, we have smoothed the power spectra with the Savgol routine in python³.

4 Cross-correlations

Cross-correlation power spectra can be found in Figure 2. First, we focus on the deflection angles. The autocorrelation of $\cos\theta_\nu$ shows a maximum for large scales around $\ell \sim 10$. This is consistent with what has been found in [7], where it has been shown that the deflection reaches its maximum at the super-cluster scales. We will comment on this in a few lines. As it was said before, the distribution of $\cos\theta_\nu$ is anti-correlated with the rest of the studied quantities. Paying attention to the first three panels in the last row of Figure 2, we see that the cross-correlation power spectra of $\cos\theta_\nu$ with the CDM and neutrino density contrast distributions, $\delta_{\Sigma_{\text{CDM}}}$ and δ_{Σ_ν} , peak at $\ell \sim 10$, and its cross-spectra with the neutrino velocity v_ν/c , at $\ell \sim 5$. It is worth nothing that, even though they peak at the same scale, the cross-correlation between $\cos\theta_\nu$ and $\delta_{\Sigma_{\text{CDM}}}$ is larger than the cross-correlation between $\cos\theta_\nu$ and δ_{Σ_ν} , and also larger than the $\cos\theta_\nu$ autocorrelation. This hints that a combination of weak-lensing maps and Ptolemy-like experiments should be sensitive to this very distinctive feature. The cross-correlation with neutrino density and velocity are scale invariant for $\ell > 20$.

Because of the small mass of neutrino particles in the simulation ($\Sigma m_\nu = 0.16$ eV), it is difficult for neutrinos to cluster at small scales. Cosmic neutrinos stream freely since they decoupled one second after the Big Bang with a frozen Fermi-Dirac momentum distribution. The momentum distribution is translated into velocity distribution through the neutrino mass, so the lower the mass the higher the thermal dispersion of neutrinos which results in clustering at increasingly larger scales. This is reflected in how δ_{Σ_ν} autocorrelation, and its cross-correlation with $\delta_{\Sigma_{\text{CDM}}}$, both peak at large scales, i.e. $\ell \sim 15$ and $\ell \sim 15$, respectively. This feature is also visible in the autocorrelation of v_ν/c where the power spectrum peaks at even larger, i.e. $\ell \sim 2$. In the same way as for angles, the signal from the cross-correlation of v_ν/c with $\delta_{\Sigma_{\text{CDM}}}$ or δ_{Σ_ν} is larger than the autocorrelation.

Finally, if we pay attention to the CDM density contrast we see how the autocorrelation power spectrum of $\delta_{\Sigma_{\text{CDM}}}$ peaks at smaller scales, i.e. large multipoles, $\ell \sim 1500$. This result agrees with the features we see in the $\delta_{\Sigma_{\text{CDM}}}$ map. This map, top left panel in Figure 1, shows the typical large-scale structure of the Universe full of vast galaxy filaments and voids spanning incredibly large distances, consequence of the higher clustering of CDM. By contrast, the δ_{Σ_ν} map, bottom left panel in Figure 1, shows a more diffuse matter distribution which translate in a power spectrum peaking at $\ell \sim 8$.

It is worth exploring in detail the cross-correlation of the neutrino field with the CDM by using an actual observable of the latter. In this case, we have chosen to construct a weak lensing convergence map, where sources are distributed via a $n(z)$ distribution, which peaks at about $z = 0.5$. The shape of the $n(z)$ and parameters are taken from the galaxy selection function expected for the photometric *Euclid* survey [42, 43]:

$$n(z) \propto \left(\frac{z}{z_0}\right)^\beta \exp\left[-\left(\frac{z}{z_0}\right)^\gamma\right], \quad (4.1)$$

where $\beta = 2$, $\gamma = 1.5$, $z_0 = z_m/\sqrt{2}$ and $z_m = 0.5$. This effective, WL map related to a source galaxy distribution can be computed as in Ref. [44] from the lightcone following the procedure

³https://docs.scipy.org/doc/scipy/reference/generated/scipy.signal.savgol_filter.html

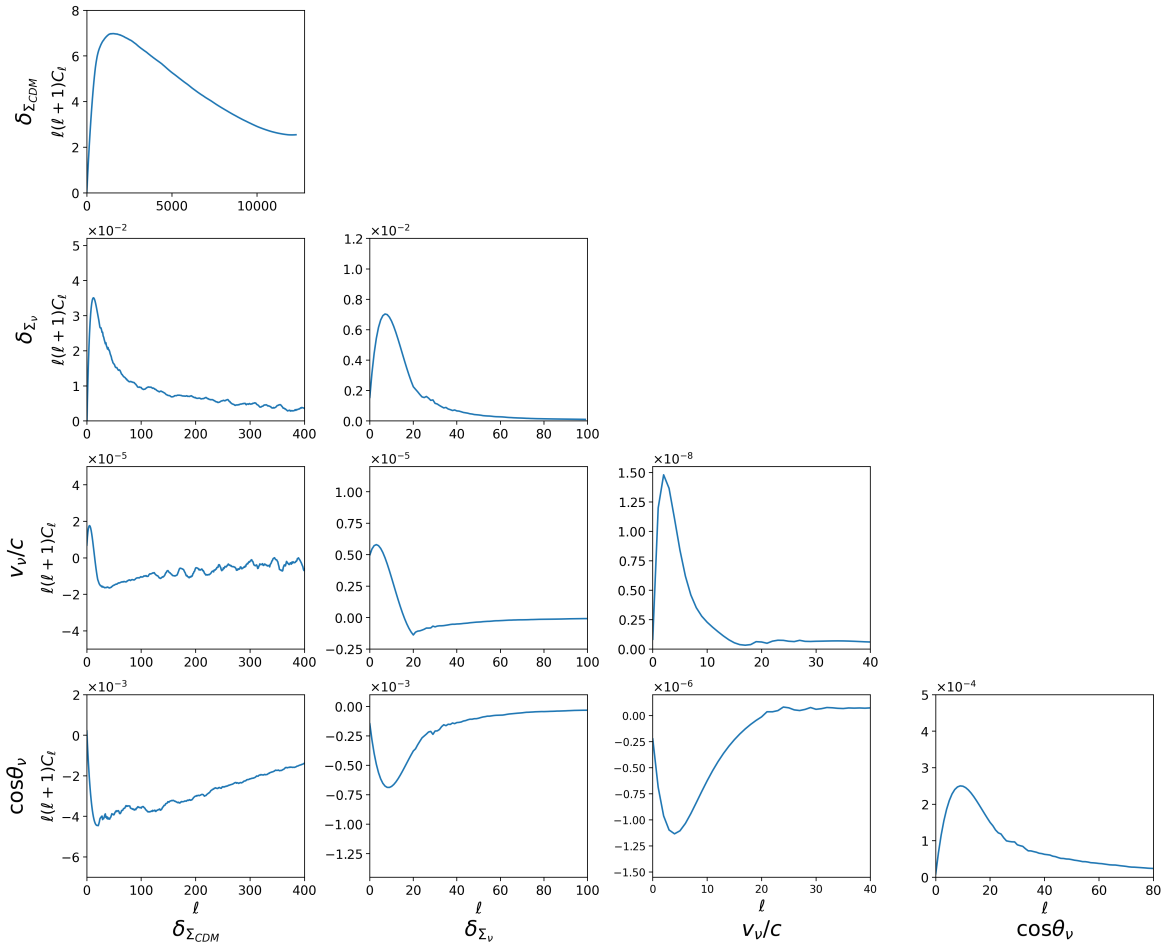


Figure 2: Cross-correlation power spectra (off-diagonal panels) along with autocorrelation power spectra (diagonal panels) for the maps shown in Figure 1.

described in [21, 34]. Since our maps (neutrino velocities and angles, matter overdensities, etc.) are constructed in a comoving volume of $(500h^{-1}\text{Mpc})^3$, this observable can maximise the cross-correlation with the neutrino fields rather than - for instance - the CMB lensing potential field, which has a broader kernel in redshift. Results for the auto-correlation for the WL map are shown in Fig. 3b. As expected, it shows the standard scale dependence for the WL signal [21, 27, 34]. The cross-correlations with the neutrino variables are shown in Fig. 4; let us notice that the $\cos\theta_\nu$ seems to anti-correlate with this effective WL field as it happens also with the CDM field. These cross-correlation power spectra peak at large scales, i.e. small ℓ , as those in Fig. 2.

We emphasise again that, also in the case of WL maps, the cross-correlations with neutrino quantities are larger than the auto-correlations for all variables studied. So we look at the cross-correlations between neutrinos and CDM as the most promising observables for future experimental surveys.

5 Conclusions

We have cross-correlated the $C\nu B$ overdensity, velocity modulus and cosine of deflection angle maps between them and with CDM overdensity and WL convergence maps, in a full-sky picture where the observer is placed at the centre. To do so, we have used the new high-resolution DEMNUni simulations that contain 2048^3 particles of each type (CDM and neutrinos) in a comoving volume of $(500h^{-1}\text{Mpc})^3$. The simulations used consider a degenerate neutrino mass scenario with three active neutrinos of $\Sigma m_\nu = 0.16\text{eV}$. The resulting maps have a pixel resolution of 0.85 arcmin. To compute the deflection angle of neutrinos we have used the same recipe as in [6, 7], i.e. calculating the angle of deflection as the angle between neutrino velocity vectors at $z = 3$ and $z = 0$.

Our results are perfectly consistent with the theoretical expectations. One of this is that CDM overdensity power spectrum peaks at smaller scales (larger multipoles) than the neutrino overdensity power spectrum because of the higher clustering of CDM. We have obtained very low auto and cross-correlation spectra for the neutrino velocity, as it was also expected, because of the large thermal velocity of cosmic neutrinos with such a low mass. Regarding the deflection angles, we have obtained a larger signal in the cross-correlation of this variable with CDM overdensity than in the cross-correlation between neutrino velocity and CDM overdensity. One of the main results is that the $C\nu B$ cross-correlations have more signal than the auto-correlations, specially in the cross-correlations with CDM overdensity, where the spectra amplitudes are three times larger than in the cross-correlations with neutrino overdensity.

We have examined the cross-correlation between the $C\nu B$ and an effective WL map obtained using the Euclid satellite specifications. This cross-correlation serves as an example of how to explore the angular dependence of $C\nu B$ signals using observable fields in modern surveys, like the Euclid mission. By demonstrating the angular dependence of these signals and identifying their maxima, this approach provides valuable insights into the nature of neutrinos through observations of the sky.

For the first time, high-fidelity cross-correlation between neutrinos and CDM maps have been shown in this paper, revealing the cosmological scales where any cross-correlation between them may occur. Once the technology to probe these cosmological probes becomes

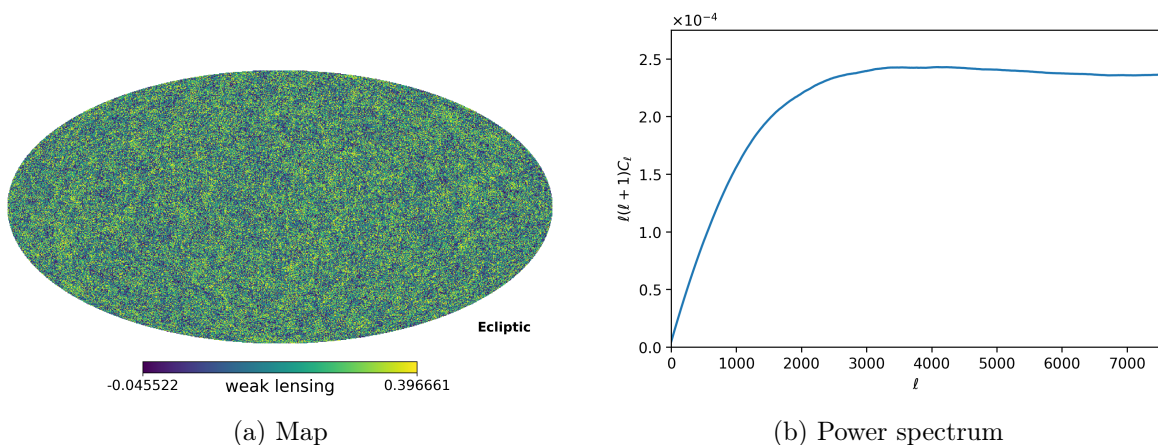


Figure 3: WL map constructed as described in the text and the corresponding power spectrum.

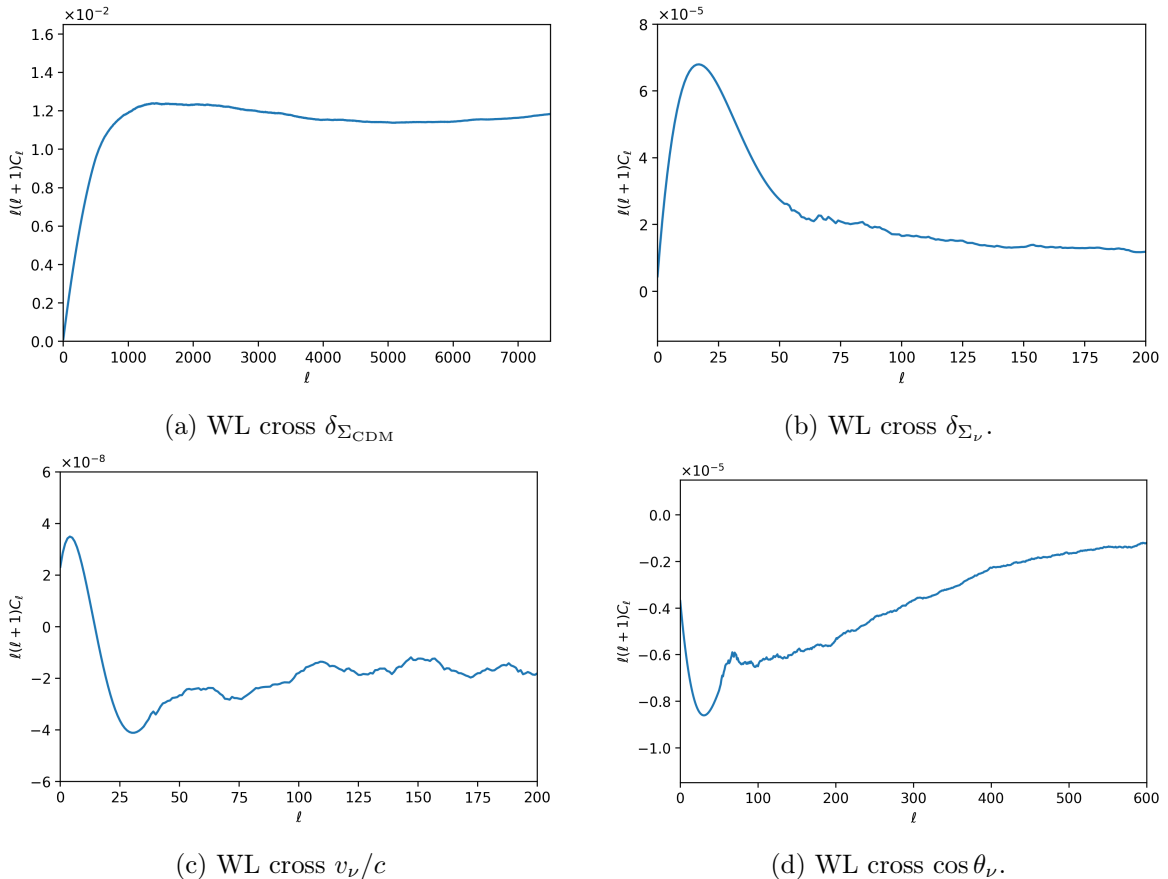


Figure 4: WL cross-correlation power spectra with different neutrino variables and the CDM itself. The cross-correlation spectra found in this case shows features similar to the one that cross-correlates the dark matter. This is expected as the weak lensing convergence is basically a re-weighting of the dark matter distribution given a $n(z)$.

available, examining these maps will enable us to confirm the detection of the cosmic neutrino background and facilitate its measurements as happens e.g. also for the Integrated Sachs-Wolfe effect of CMB when exploiting its correlation with galaxies.

Acknowledgments

The DEMNUni simulations were carried out in the framework of “The Dark Energy and Massive Neutrino Universe” project, using the Tier-0 IBM BG/Q Fermi machine, the Tier-0 Intel OmniPath Cluster Marconi-A1 and Marconi-100 of the Centro Interuniversitario del Nord-Est per il Calcolo Elettronico (CINECA). CC acknowledges a generous CPU and storage allocation by the Italian Super-Computing Resource Allocation (ISCRA) as well as from the coordination of the “Accordo Quadro MoU per lo svolgimento di attività congiunta di ricerca Nuove frontiere in Astrofisica: HPC e Data Exploration di nuova generazione”, together with storage from INFN-CNAF and INAF-IA2. This work was supported by the “Center of Excellence Maria de Maeztu 2020-2023” award to the ICCUB (CEX2019-000918-M) funded by MCIN/AEI/10.13039/501100011033. Funding for the work of RJ was partially provided by project PID2022-141125NB-I00. AG would also like to thank Martin Reinecke for

many useful discussions about some technical aspects during the early stages of this work. MC is partially supported by the 2023/24 “Research and Education” grant from Fondazione CRT. The OAVdA is managed by the Fondazione Clément Fillietroz-ONLUS, which is supported by the Regional Government of the Aosta Valley, the Town Municipality of Nus and the “Unité des Communes valdôtaines Mont-Émilium”.

References

- [1] PTOLEMY collaboration, *Neutrino physics with the PTOLEMY project: active neutrino properties and the light sterile case*, *JCAP* **07** (2019) 047 [[1902.05508](#)].
- [2] A. D. Dolgov, *Neutrinos in cosmology*, *Phys. Rept.* **370** (2002) 333 [[hep-ph/0202122](#)].
- [3] J. Lesgourgues and S. Pastor, *Massive neutrinos and cosmology*, *Physics Reports* **429** (2006) 307 [[astro-ph/0603494](#)].
- [4] A. D. Dolgov, *Cosmology and neutrino properties*, *Physics of Atomic Nuclei* **71** (2008) 2152?2164 [[0803.3887](#)].
- [5] A. J. Long, C. Lunardini and E. Sabancilar, *Detecting non-relativistic cosmic neutrinos by capture on tritium: phenomenology and physics potential*, *JCAP* **08** (2014) 038 [[1405.7654](#)].
- [6] B. Hernandez-Molinero, R. Jimenez and C. Pena-Garay, *Distinguishing Dirac vs. Majorana neutrinos: a cosmological probe*, *JCAP* **08** (2022) 038 [[2205.00808](#)].
- [7] B. Hernandez-Molinero, C. Carbone, R. Jimenez and C. P. Garay, *Cosmic background neutrinos deflected by gravity: DEMNUni simulation analysis*, *Journal of Cosmology and Astroparticle Physics* **2024** (2024) 006.
- [8] E. Roulet and F. Vissani, *On the capture rates of big bang neutrinos by nuclei within the Dirac and Majorana hypotheses*, *JCAP* **10** (2018) 049 [[1810.00505](#)].
- [9] DESI Collaboration, A. G. Adame, J. Aguilar, S. Ahlen, S. Alam, D. M. Alexander et al., *DESI 2024 VI: Cosmological Constraints from the Measurements of Baryon Acoustic Oscillations*, *arXiv e-prints* (2024) [arXiv:2404.03002](#) [[2404.03002](#)].
- [10] F. Simpson, R. Jimenez, C. Pena-Garay and L. Verde, *Strong Bayesian evidence for the normal neutrino hierarchy*, *JCAP* **2017** (2017) 029 [[1703.03425](#)].
- [11] R. Jimenez, C. Pena-Garay, K. Short, F. Simpson and L. Verde, *Neutrino masses and mass hierarchy: evidence for the normal hierarchy*, *JCAP* **2022** (2022) 006 [[2203.14247](#)].
- [12] M. Goeppert-Mayer, *Double beta-disintegration*, *Phys. Rev.* **48** (1935) 512.
- [13] W. H. Furry, *On transition probabilities in double beta-disintegration*, *Phys. Rev.* **56** (1939) 1184.
- [14] C. Carbone, M. Petkova and K. Dolag, *DEMNUi: ISW, Rees-Sciama, and weak-lensing in the presence of massive neutrinos*, *JCAP* **2016** (2016) 034 [[1605.02024](#)].
- [15] E. Castorina, C. Carbone, J. Bel, E. Sefusatti and K. Dolag, *DEMNUi: the clustering of large-scale structures in the presence of massive neutrinos*, *JCAP* **7** (2015) 043 [[1505.07148](#)].
- [16] M. Moresco, F. Marulli, L. Moscardini, E. Branchini, A. Cappi, I. Davidzon et al., *The VIMOS Public Extragalactic Redshift Survey (VIPERS) . Exploring the dependence of the three-point correlation function on stellar mass and luminosity at $0.5 < z < 1.1$* , *Astron. Astrophys.* **604** (2017) A133 [[1603.08924](#)].
- [17] M. Zennaro, J. Bel, J. Dossett, C. Carbone and L. Guzzo, *Cosmological constraints from galaxy clustering in the presence of massive neutrinos*, *Mon. Not. Roy. Astron. Soc.* **477** (2018) 491 [[1712.02886](#)].

- [18] R. Ruggeri, E. Castorina, C. Carbone and E. Sefusatti, *DEMNUni: massive neutrinos and the bispectrum of large scale structures*, *JCAP* **2018** (2018) 003 [1712.02334].
- [19] J. Bel, A. Pezzotta, C. Carbone, E. Sefusatti and L. Guzzo, *Accurate fitting functions for peculiar velocity spectra in standard and massive-neutrino cosmologies*, *Astron. Astrophys.* **622** (2019) A109 [1809.09338].
- [20] G. Parimbelli, S. Anselmi, M. Viel, C. Carbone, F. Villaescusa-Navarro, P. S. Corasaniti et al., *The effects of massive neutrinos on the linear point of the correlation function*, *JCAP* **2021** (2021) 009 [2007.10345].
- [21] G. Parimbelli, C. Carbone, J. Bel, B. Bose, M. Calabrese, E. Carella et al., *DEMNUni: comparing nonlinear power spectra prescriptions in the presence of massive neutrinos and dynamical dark energy*, *JCAP* **2022** (2022) 041 [2207.13677].
- [22] M. Guidi, A. Veropalumbo, E. Branchini, A. Eggemeier and C. Carbone, *Modelling the next-to-leading order matter three-point correlation function using FFTLog*, *JCAP* **2023** (2023) 066 [2212.07382].
- [23] P. Baratta, J. Bel, S. Gouyou Beauchamps and C. Carbone, *COVMOS: a new Monte Carlo approach for galaxy clustering analysis*, *arXiv e-prints* (2022) arXiv:2211.13590 [2211.13590].
- [24] S. Gouyou Beauchamps, P. Baratta, S. Escoffier, W. Gillard, J. Bel, J. Bautista et al., *Cosmological inference including massive neutrinos from the matter power spectrum: biases induced by uncertainties in the covariance matrix*, *arXiv e-prints* (2023) arXiv:2306.05988 [2306.05988].
- [25] E. Carella, C. Carbone, M. Zennaro, G. Girelli, M. Bolzonella, F. Marulli et al., “Demnuni: The galaxy-halo connection in the presence of dynamical dark energy and massive neutrinos.”.
- [26] M. Roncarelli, C. Carbone and L. Moscardini, *The effect of massive neutrinos on the Sunyaev-Zel’dovich and X-ray observables of galaxy clusters*, *Mon. Not. Roy. Astron. Soc.* **447** (2015) 1761 [1409.4285].
- [27] G. Fabbian, M. Calabrese and C. Carbone, *CMB weak-lensing beyond the Born approximation: a numerical approach*, *JCAP* **2018** (2018) 050 [1702.03317].
- [28] C. D. Kreisch, A. Pisani, C. Carbone, J. Liu, A. J. Hawken, E. Massara et al., *Massive neutrinos leave fingerprints on cosmic voids*, *Mon. Not. Roy. Astron. Soc.* **488** (2019) 4413 [1808.07464].
- [29] N. Schuster, N. Hamaus, A. Pisani, C. Carbone, C. D. Kreisch, G. Pollina et al., *The bias of cosmic voids in the presence of massive neutrinos*, *JCAP* **2019** (2019) 055 [1905.00436].
- [30] G. Verza, A. Pisani, C. Carbone, N. Hamaus and L. Guzzo, *The void size function in dynamical dark energy cosmologies*, *JCAP* **2019** (2019) 040 [1906.00409].
- [31] G. Verza, C. Carbone and A. Renzi, *The Halo Bias inside Cosmic Voids*, *Astrophys. J. Lett.* **940** (2022) L16 [2207.04039].
- [32] G. Verza, C. Carbone, A. Pisani and A. Renzi, *DEMNUni: disentangling dark energy from massive neutrinos with the void size function*, *arXiv e-prints* (2022) arXiv:2212.09740 [2212.09740].
- [33] P. Vielzeuf, M. Calabrese, C. Carbone, G. Fabbian and C. Baccigalupi, *DEMNUni: the imprint of massive neutrinos on the cross-correlation between cosmic voids and CMB lensing*, *JCAP* **2023** (2023) 010 [2303.10048].
- [34] V. Cuozzo, C. Carbone, M. Calabrese, E. Carella and M. Migliaccio, *DEMNUni: cross-correlating the nonlinear ISWRS effect with CMB-lensing and galaxies in the presence of massive neutrinos*, *arXiv e-prints* (2023) arXiv:2307.15711 [2307.15711].

- [35] M. Zennaro, J. Bel, F. Villaescusa-Navarro, C. Carbone, E. Sefusatti and L. Guzzo, *Initial conditions for accurate N-body simulations of massive neutrino cosmologies*, *Mon. Not. Roy. Astron. Soc.* **466** (2017) 3244 [[1605.05283](#)].
- [36] Planck Collaboration, P. A. R. Ade, N. Aghanim, C. Armitage-Caplan, M. Arnaud, M. Ashdown et al., *Planck 2013 results. XVI. Cosmological parameters*, *Astron. Astrophys.* **571** (2014) A16 [[1303.5076](#)].
- [37] C. Carbone, C. Baccigalupi, M. Bartelmann, S. Matarrese and V. Springel, *Lensed CMB temperature and polarization maps from the Millennium Simulation*, *Mon. Not. Roy. Astron. Soc.* **396** (2009) 668 [[0810.4145](#)].
- [38] M. Calabrese, C. Carbone, G. Fabbian, M. Baldi and C. Baccigalupi, *Multiple lensing of the cosmic microwave background anisotropies*, *JCAP* **3** (2015) 049 [[1409.7680](#)].
- [39] G. Fabbian, M. Calabrese and C. Carbone, *CMB weak-lensing beyond the Born approximation: a numerical approach*, *JCAP* **2018** (2018) 050 [[1702.03317](#)].
- [40] S. Hilbert, A. Barreira, G. Fabbian, P. Fosalba, C. Giocoli, S. Bose et al., *The accuracy of weak lensing simulations*, *Mon. Not. Roy. Astron. Soc.* **493** (2020) 305 [[1910.10625](#)].
- [41] K. M. Górski, E. Hivon, A. J. Banday, B. D. Wandelt, F. K. Hansen, M. Reinecke et al., *HEALPix: A Framework for High-Resolution Discretization and Fast Analysis of Data Distributed on the Sphere*, *Astrophys. J.* **622** (2005) 759 [[astro-ph/0409513](#)].
- [42] R. Laureijs, J. Amiaux, S. Arduini, J. L. Auguères, J. Brinchmann, R. Cole et al., *Euclid Definition Study Report*, *arXiv e-prints* (2011) [arXiv:1110.3193](#) [[1110.3193](#)].
- [43] Euclid Collaboration, A. Blanchard, S. Camera, C. Carbone, V. F. Cardone, S. Casas et al., *Euclid preparation. VII. Forecast validation for Euclid cosmological probes*, *Astron. Astrophys.* **642** (2020) A191 [[1910.09273](#)].
- [44] M. Bartelmann and P. Schneider, *Weak gravitational lensing*, *Phys. Reports* **340** (2001) 291 [[astro-ph/9912508](#)].